

Partial discharge detection and localization using Software

Defined Radio

Abstract

Partial Discharge (PD) occurs when insulation containing voids is subjected to high voltage (HV). If left untreated PD can degrade insulation until, eventually, catastrophic insulation failure occurs. The detection of PD current pulses, however, can allow incipient insulation faults to be identified, located and repaired prior to plant failure. Traditionally PD is detected using galvanic contact methods or capacitive/inductive coupling sensors. This article discusses the use of Software Defined Radio (SDR) for PD detection and localization, and presents proof of principle experimental results that suggest SDR can provide a simple and reliable solution for PD-based monitoring of HV insulation integrity.

Introduction to Partial Discharge

Insulation of HV equipment is vital for its efficient operation. However, in most HV power systems, degradation and breakdown of insulation is a major challenge, [1]. Partial discharge in electrical systems indicates the deterioration of insulating materials. Sometimes this is just an air or gas-filled void in a solid or liquid dielectric insulator. When insulators are subjected to intense electrical stresses in the presence of impurities, PD is likely to occur. If two insulating materials with different dielectric permittivity are subjected to a voltage, the resultant electric field is greater in the region of smaller permittivity (e.g. in a void). Electrical breakdown can occur in this region without occurring elsewhere. Figure 1 shows an equivalent circuit for the partial discharge phenomenon where a capacitive voltage divider is formed between the two regions. Repeated partial discharge further damages the insulation by causing treeing and may eventually result in complete catastrophic discharge, i.e. flashover. Thus PD is defined as a localized electrical discharge that only partially bridges the insulation between conductors.

Current pulses typically last for a few nanoseconds. However, these repeated discharges can eventually lead to full discharges that totally destroy the insulating material resulting in catastrophic failures of power equipment, [2]. It is imperative that PD occurrence, modes and types be studied in order to assist in the preventive maintenance and effective management of HV equipment, [1-3]. PD can also appear as localized dielectric discharges developing in a secluded area of electric insulation subjected to an electrical field stress. It can occur in virtually any part of the insulation where electric field precipitates the breakdown of that particular area of the insulating material, e.g. in cables, switchgear, generators, transformers, etc. Therefore, PD measurements must be performed on a regular basis to monitor the integrity of insulating materials. Several methods have been employed for partial discharge detection, and each of these methods has its advantages and disadvantages as shown in Table 1. Most PD detection methods are only suitable to be used in the laboratory except for the UHF radiometric method, which is not a particularly inexpensive method, [4]. The UHF radiometric method is using a wideband antenna coupled to a costly fast-sampling oscilloscope (time domain variant) or spectrum analyzer (frequency domain variant) in order to remotely detect and localize PD pulses. However, SDR technology brought the cost of the UHF PD detection method down to affordable levels. The IEC 60270 and IEC 62478 standards present common techniques for PD detection, [5-6]. These techniques include galvanic contact measurement methods, radiometric methods, and acoustic emission based methods. Traditional galvanic contact measurement methods usually rely on capacitive or inductive coupling to detect electrical PD pulses, while acoustic methods utilize highly sensitive directional microphones to detect the sound of these pulses. On the other hand, the promising free-space radiometric method of PD measurement uses an antenna and a fast sampling oscilloscope or simpler radiometers, or, alternatively, a spectrum analyzer to receive wideband electromagnetic signals radiated in the VHF and UHF bands by the short-duration transient PD pulses. It is important to localize PD with some spatial

accuracy in order to identify faulty components in an HV substation and thus prevent catastrophic failures. With typical size HV equipment, a localization accuracy of one meter is adequate in practice.

Figure 2 shows a PD WSN (Wireless Sensor Network) that can be used for the continuous monitoring of PD activity in large-scale power station. The PD monitoring WSN is composed of sensor nodes which communicate via a central HUB. The sensor nodes are arranged in a grid array, spaced approximately 20 to 30 m apart. Each node communicates to the central HUB via a robust industrial standard wireless HART and may transmit data via intermediate nodes to the central HUB in order to ensure no data is lost. The resulting electromagnetic signal due to a PD event propagates away from the source. This signal is received by sensor nodes in the immediate vicinity of the PD source. The nodes measure the intensity of the PD with relation to the inverse power law due to distance. Therefore, a location algorithm based on received signal strength (RSS) can be used to locate the source of PD, an estimation error is proposed to be less than 1 meter, [7]. Individual sensor nodes are usually hardware based radiometers, [8]. Recently, however, cost-effective alternative methods to detect and monitor PD activity using wireless technology have become possible using broadband radiometers, [9-13]. The development of SDR offers new opportunities for wireless PD detection and monitoring and preliminary results can be found in [14-15]. In this article the use of SDR for PD detection and localization is discussed. It should be mentioned that this technique has been successfully applied in the Tata Steel, Port Talbot, UK, industrial complex in 2017, [16]. The remainder of the article is organized as follows: after a brief introduction to PD, an analysis of existing spectrum measurement platforms is presented. Then, an SDR-based PD detection system suitable for use in an HV substation is described, followed by a section on localization algorithms. Finally, the article main points are summarized in the conclusion section.

Analysis of existing spectrum analysis platforms – Spectrum analyzers and SDRs

In this section a range of sensing solutions are presented, including complex and expensive spectrum analyzers and simpler but cheaper SDR-based WSNs (Wireless Sensor Networks). Most modern spectrum analyzers have one of two principal operating modes: Fast Fourier Transform (FFT) and swept mode, [17-19]. Some spectrum analyzers combine the FFT and swept modes. They obtain several FFTs at different center frequencies and then combine them to produce one full spectrum sweep. This is sometimes referred to as swept-FFT mode. The FFT-based analyzer has one main advantage; one operation can enable you to look at a spectrum on a broader range. However, the acquisition of a batch of samples followed by a step that involves processing is required in the FFT mode and the analyzer might miss some events while in the processing step. This problem can be solved and seamless measurements can be obtained if the analyzer processing speed is faster than the acquisition speed, and if the sample acquisition step and the sample processing step occur in parallel. Spectrum analyzers that have the capability of seamless measurements are called real-time spectrum analyzers, [17-18]. The swept-FFT mode is illustrated in Fig. 3, [18].

On the other hand, the Universal Software Radio Peripheral USRP device (originally developed by Ettus Research) is a low-cost and high-speed device [19]. SDR platforms allow basic traditional radio functions, which include filtering, encoding and decoding, to be transferred from hardware to software. The USRP consists of a Radio Frequency (RF) section, an Intermediate Frequency (IF) section, and a baseband section. RF and IF functions are performed on the USRP and baseband functions are performed on a host computer. These sections are implemented on two boards; a plug-in daughter board (RF), and a fixed motherboard (IF). Fig. 4. shows the USRP system block diagram. USRPs can be reconfigured to realize a desired specification using software. All the modules make use of a USRP Hardware Driver (UHD) software package. UHD is compatible with Windows, Linux and

MacOs and has functions that can control parameters such as frequency, gain and sample rate. The USRP N200 has an IF bandwidth of 50 MHz with 8 bit samples and an IF bandwidth of 25 MHz with 16 bit samples. ADCs are 14 bits at 100 MSa/s and DACs are 16 bits at 400 MSa/s. The Gigabit Ethernet interface of the USRP allows high-speed streaming capability up to 50 MSa/s in both directions (8-bit samples), [19]. Table 2 shows a comparison of SDR-based UHF sensing against a conventional portable spectrum analyser solution.

Partial Discharge Detection

An experimental apparatus is shown in Fig. 5. The PD emulator is located inside a wooden box with a perspex door to prevent accidental contact with the HV terminals. The detector comprises a USRP N200 transceiver, a laptop and a wideband biconical antenna [15-16]. The USRP N200 is programmed to measure the spectrum in the 50-800 MHz band while the useful frequency range of the biconical antenna is 50MHz to 1 GHz, and it has a nominal impedance of 50 Ohms. A PD signal is generated by applying a high voltage of 15 kVrms to a PD floating-electrode emulator. The lower electrode of the PD emulator is connected to the AC power supply while the upper electrode is connected to earth. More information on the experimental setup can be found in [22]. PD signals were simultaneously recorded using a spectrum analyzer for validations purposes. Measurements were taken with (i) the HV power supply turned off to obtain the spectrum in the absence of PD, and (ii) with the power supply turned on to obtain the spectrum in the presence of PD. It should be noted that USRP measured absolute power levels are not calibrated.

Fig. 6 shows the USRP measured spectrum using USRP N200 and spectrum analyzer when the PD signal is absent and when it is present. The spectra were recorded at a distance of 3 meters from the PD source. The power spectrum is dominated by lower frequencies in the range of 50-500 MHz. In particular interference from TV broadcast signals is present in the frequency

band of 550-720 MHz, and there is also interference from communication signals at approximately 225 MHz, and interference from mobile communication signals in the 790-800 MHz band (4G-LTE). In these experiments, a significant increase in the amplitude of the measured spectra of the order of 10 to 20dB is observed in the presence of PD activity. Naturally, spectrum analyzer results look clearer and more detailed. Furthermore, the spectrum analyzer has a lower noise floor and a better sensitivity as expected from a high-end instrument. However, post-filtering USRP results in Fig. 7 seem to be very satisfactory for a relatively low-cost device.

PD detection in an electrical power station

PD detection can be challenging in the presence of strong electromagnetic interference. Discrete Spectral Interference (DSI) arises from mobile communications systems and TV/radio broadcasting and Private Mobile Radio (PMR) devices in the VHF and UHF bands. Interference may also be caused by power switching circuits from surrounding devices and from the PD detection system itself, [9-13].

It is worth mentioning here that to detect the PD signal and localize it in an electrical power station, the following procedure is followed:

1. Scan the frequency band of 50-800 MHz to set the noise floor in the surrounding area of the electrical plant, not very far away from the electrical equipment, at around 50-100 meters. The spectrum obtained is the noise floor or, more accurately, the noise background, and it is considered as reference for the rest of the scans. This scan should be repeated several times in order to make the measurements more accurate.
2. Scan the same frequency band 50-800 MHz at least at three different locations near the electrical equipment several times just after finishing the first scan. This is to ensure that the PD signal does not significantly change over time.

3. Finally, after scanning the noise background and the PD signal, and after signal processing to reduce noise, the PD source can be localized adopting a specific localization algorithm.

Various noise removal approaches are adopted to reduce noise and external interference. Median and moving average filters are simple and powerful denoising methods. They can filter out the spikes that are caused by interferer signals from radio communication systems as well as impulsive noise. To remove these spikes and obtain reliable and clean spectra, first the median filter was applied followed by a moving average filter. The final results, after applying both filters for the PD signal and noise, are shown in Fig. 7 (bottom). Comparing it to the spectra shown in Fig. 7 (top), it can be observed that the results are clearer and the spikes have been removed, however, some very strong interference is still present caused by TV broadcasting and mobile communications in the frequency range of 450-800 MHz. This frequency band is then removed to avoid interferences and the new calculated band is reduced to 50-450 MHz. It is commonly known that most of PD energy is concentrated at lower frequencies, thus the removed band is not expected to have a negative impact on diagnosis. The new reduced PD band is shown in Fig. 8. Subsequently, an integration operation over frequency is performed in order to obtain the average power at each location in milliWatts.

Partial discharge localization

Efficient PD detection and monitoring cannot be completed until the PD source is localized, thus the positioning phase is very important. Afterwards, by localizing the PD source, the required maintenance or action can be performed. Several localization algorithms can be adopted. Examples of algorithms are: time of arrival (TOA), angle of arrival (AOA), time difference of arrival (TDOA), received signal strength (RSS), etc., [20-24]. Recently the RSS algorithm approach has been preferred for indoors and outdoors localization due to cost-

effectiveness because it does not require the employment of antenna arrays or synchronization, thus hardware cost is minimized, [23-24].

Received signal strength (RSS) localization algorithm

Received signal strength is a simple and cost effective algorithm as there is no need to install additional hardware and software, [7]. A lower quality of communication between the receiver and the transmitter is mostly caused by a lower received signal strength. RSS provides information about the distance between the transmitter and the source. This distance is obtained by converting the received signal strength into a distance using the path-loss exponent model as shown in eq. (1):

$$R_i = R_o - 10n \log_{10} \left(\frac{d_i}{d_{ref}} \right) \quad (1)$$

Where, R_i is proportional to the received signal power (in dBm); R_o is the radiated power of the PD source (in dBm); d_i is the distance between the i^{th} receiver and the PD source; d_{ref} is a reference distance; n is the path loss exponent ($n = 2$ for free space propagation).

Using multiple receiver nodes can allow trilateration or even multilateration for multiple source location. The accuracy of the estimated source location is the main issue because of the heterogeneous nature of the radio propagation environment. Therefore, the challenge here is how to deal with the anonymity of the propagation parameters, the unknown radiated power, and the unknown path loss index n that can also vary from one node to another depending on the nature of the propagation environment in that link.

According to the equation above, the received power or the received signal strength is converted into distance, and because of having unknown parameters like the radiated power and the path loss index, the use of linear approximation is necessary. RSS is a simple and cost effective approach but its main disadvantage is low accuracy especially at the corners of the measurement grid. In order to improve accuracy more nodes need to be deployed and a finer

grid has to be used. Regarding the unknown parameters, the radiated power is eliminated from the calculations and only relative received powers are used. On the other hand, the path loss index is estimated by the algorithm, [7, 24]. Expected uncertainties in distance calculations are of approximately 1 meter. Fig. 9. presents a flowchart of the algorithm used. The algorithm steps are:

- (i) initially assume a plausible path-loss index (e.g. $n = 2$, free space propagation).
- (ii) calculate the received power ratios at any two nodes to find the locus of possible source locations.
- (iii) establish an initial estimate of source location using intersecting loci from all measurements node pairs.
- (iv) calculate an improved estimate of source location using different values of path-loss indices n between 1 and 5 with a step of 0.01. Iterate to converge on a final source location estimate and an average path-loss index n .

It is worth mentioning that the error should be less than 1 meter to stop the algorithm. For the RSS algorithm a minimum of three nodes are required, but in practice at least 6 nodes have to be used to obtain satisfactory results. Accuracy generally improves by increasing the number of nodes. However, the main challenge is the optimization of the estimated path-loss index n .

The localization results

In this experiment the same receiver was used to record results in 6 different locations. However, in a permanently deployed system 6 receivers would be required. The power values obtained at every node are entered into the MATLAB code in order to localize the source. The localization results are shown in Fig. 10. The estimation error is 1.3 m, and comparing it to the proposed estimation error that is 1 m, it can still be considered acceptably accurate for HV

system condition monitoring purposes. The recorded power values at six locations are shown in Table 3 where the power values are in milliWatts. It is worth mentioning here that this is only a relative estimate of received power and not absolute power because the received signal power by the USRP is not calibrated as can be seen in Table 3. The computation time by the RSS algorithm for 6 nodes is very short, less than a second, however spectrum scanning can take significantly longer, of the order of tens of seconds.

The key variables that can affect the range of the SDR system are: the site location, in that the range can vary significantly from one site to another depending on the surrounding environment. Also the type of SDR device and antenna, in addition to the strength of PD signal can all affect the SDR system range. However, practical measurements have shown that the SDR localization system can detect PD signals at a maximum range of around 20m, and this is a very promising outcome of this research. Future studies will focus on increasing the range and accuracy of the SDR PD detection system.

Conclusion

In this article, after an overview of industrial PD detection systems, the SDR technique for partial discharge detection using wideband radio spectrum measurements is described. To achieve optimal performance for wideband spectrum sensing using low-cost SDR systems, some basic signal processing has to be performed. SDR-based PD detection exhibits acceptable performance as compared to conventional spectrum analyzers. Hence, it can be used as a cost-effective alternative technique for spectrum sensing and PD localization for the early detection of faulty HV equipment, thus avoiding catastrophic failures in HV substations.

Acknowledgment

The authors acknowledge the Engineering and Physical Sciences Research Council for their support of this work under grant EP/J015873/1.

References

1. H. Henao, G. Capolino, M. Fernandez, F. Filippetti, C. Bruzzese, E. Strangas, R. Pusca, J. Estima, M. Piera and S. Hedayati, "Trends in fault diagnosis for electrical machines: A review of diagnostic techniques", *IEEE Industrial Electronics Magazine*, vol. 8, no. 2, pp. 31-42, Jun. 2014.
2. M. Florkowski, "Exploitation stresses and challenges in diagnostics of electrical industrial equipment". In *2011 IEEE International Symposium on Industrial Electronics (ISIE)*, pp. 15-25, University of Technology, Gdansk, Poland, Jun. 2011.
3. D. A. Genutis, "Using partial discharge surveys to increase electrical reliability", *Annual Technical Conf. Communications and Metering*, Neta World, USA, pp. 69-73, 2002.
4. M. Yaacob, M. Alsaedi, R. Rashed, M. Dakhil, and F. Atyah. "Review on partial discharge detection techniques related to high voltage power equipment using different sensors". *Photonic sensors*, 4(4), 325-337, 2014.
5. IEC 62478. "High voltage test techniques - Measurement of partial discharges by electromagnetic and acoustic methods", Proposed Horizontal Standard, 1st ed., International Electrotechnical Commission (IEC): Geneva, Switzerland, 2016.
6. IEC 60270. "High-voltage Test Techniques: Partial Discharge Measurements," International Electrotechnical Commission (IEC), pp. 1-51, 2000.
7. U. Khan, P. Lazaridis, H. Mohamed, R. Albarracín, Z. Zaharis, R. Atkinson, C. Tachtatzis, and I. Glover "An Efficient Algorithm for Partial Discharge Localization in High-voltage System using Received Signal Strength", *Sensors*, 18(11), 4000, 2018.
8. J. M. R. De Souza Neto, E. C. T. de Macedo, J. S. da Rocha Neto, E. G. Da Costa, S. A. Bhatti, and I. A. Glover, "Partial discharge location using unsynchronized radiometer network for condition monitoring in HV substations – a proposed approach," *J. Phys.*, vol. 364, no. 1, p.012053, IOP Publishing, 2012.
9. Y. Zhang, D. Upton, A. Jaber, U Khan, B. Saeed, H. Ahmed, P. Mather, P. Lazaridis, R. Atkinson, M. Vieria and I. Glover, "Radiometric wireless sensor network monitoring of partial discharge sources in electrical substations" *Hindawi International Journal of Distributed Sensor Networks*, vol. 179, pp. 1-9, Aug. 2015.
10. P. Moore, I. Portugues and I. Glover "Radiometric location of partial discharge sources on energized high-voltage plant" *IEEE Transactions on Power Delivery*, vol. 20, no. 3, pp. 2264-2272, Jul. 2005.

11. R. Albarracín, G. Robles, J. Martínez-Tarifa, J. Ardila-Rey “Separation of sources in radiofrequency measurements of partial discharges using time–power ratio maps” *ISA transactions*, vol. 58, pp. 389-397, Sept. 2015.
12. G. Robles, M. Fresno and J. Martínez-Tarifa “Separation of radio-frequency sources and localization of partial discharges in noisy environments”. *Sensors*, vol. 15, no. 5, pp. 9882-9898, Apr. 2015.
13. R. Albarracín, A. Ardila-Rey, and A. Mas’ud “On the use of monopole antennas for determining the effect of the enclosure of a power transformer tank in partial discharges electromagnetic propagation”. *Sensors*, vol. 16, no. 2, p.148-166, Jan. 2016.
14. H. Mohamed, P. Lazaridis, U. Khan, D. Upton, B. Saeed, A. Jaber, P. Mather, D. Atkinson, K. Barlee, M. Vieira and I. Glover, “Partial discharge detection using Software Defined Radio”, *IEEE ICSAE Conf.*, Newcastle, England, Oct. 2016.
15. H. Mohamed, P. Lazaridis, Umar Khan, D. Upton, B. Saeed, A. Jaber, P. Mather, D. Atkinson, K. Barlee, M. Vieira and I. Glover, “Partial discharge detection using low cost RTL-SDR model for wideband spectrum sensing”, *IEEE ICT 2016 Conf.*, Thessaloniki, Greece, May 2016.
16. <https://www.hud.ac.uk/news/2017/november/electricitysubstationmonitoringsystemsaccessattatasteel/>
17. W. Liu, D. Pareit, E. De Poorter, and, I. Moerman, “Advanced spectrum sensing with parallel processing based on software-defined radio,” *EURASIP Journal on Wireless Commun. and Networking*, vol. 228, 2013.
18. R. W. Stewart, K. W. Barlee, D. S. W. Atkinson, L. H. Crockett, “Software Defined Radio using MATLAB & Simulink and the RTL-SDR”, 1st Ed. Published by Strathclyde Academic media, ISBN-13: 978-0-9929787-1-6, 2015.
19. Ettus Research, www.ettus.com.
20. J. M. Fresno, G. Robles, J. M. Martínez-Tarifa, and, B. G. Stewart, “Survey on the performance of source localization algorithms,” *Sensors*, vol. 17, No. 11, Nov. 2017.
21. E.T. Iorkyase, C. Tachtatzis, P. Lazaridis, I. A. Glover, and, R. C. Atkinson, “Radio location of partial discharge sources: a support vector regression approach,” *IET Science, Measurement and Technology*, vol. 12, no 2, pp. 230-236, Mar. 2018.
22. A. A. Jaber, A., P. I. Lazaridis, M. Moradzadeh, I. A. Glover, Z. D. Zaharis, M. F. Q. Vieira, M. D. Judd, and R. C. Atkinson, “Calibration of Free-Space Radiometric Partial

Discharge Measurements," *IEEE Transactions on Dielectrics and Electrical Insulation*, vol. 24, no. 5, pp. 3004-3014, Nov. 2017.

23. Y. Zhang, Y. Zhang, D. Upton, A. Jaber, H. Mohamed, U. Khan, B. Saeed, P. Mather, P. Lazaridis, R. Atkinson, M.F. Q Vieira and I Glover, " Multiple Source Localization for Partial Discharge Monitoring in Electrical Substation,"in *IEEE Loughborough Antennas & Propagation Conference (LAPC)*, Loughborough, UK, 2015.
24. Y. Xu, Y. Xu, Z. Jianguo and P. Zhang. "RSS-based source localization when path-loss model parameters are unknown," *IEEE Communications Letters*, vol. 18, no 6, pp. 1055-1058, Apr. 2014.

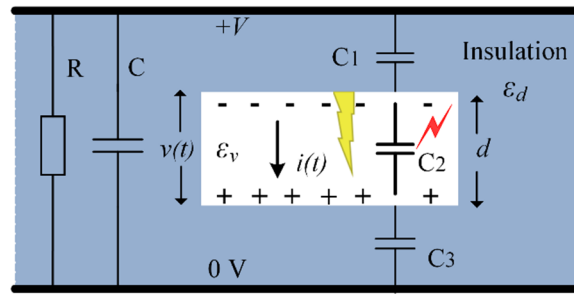


Fig. 1. An equivalent circuit for the partial discharge phenomenon.

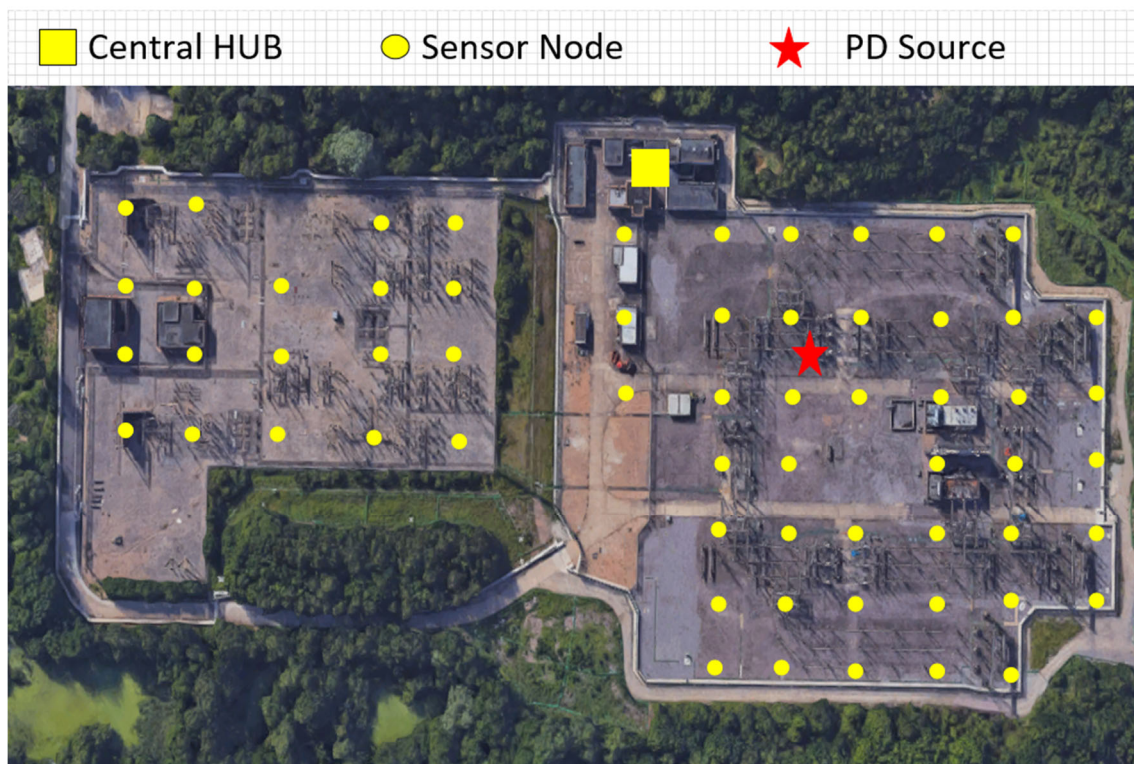


Fig. 2. A PD Wireless Sensor Network in an electricity power station.

Individual ‘tunes’ of the SDR devices will return bands of spectral information f_s Hz wide

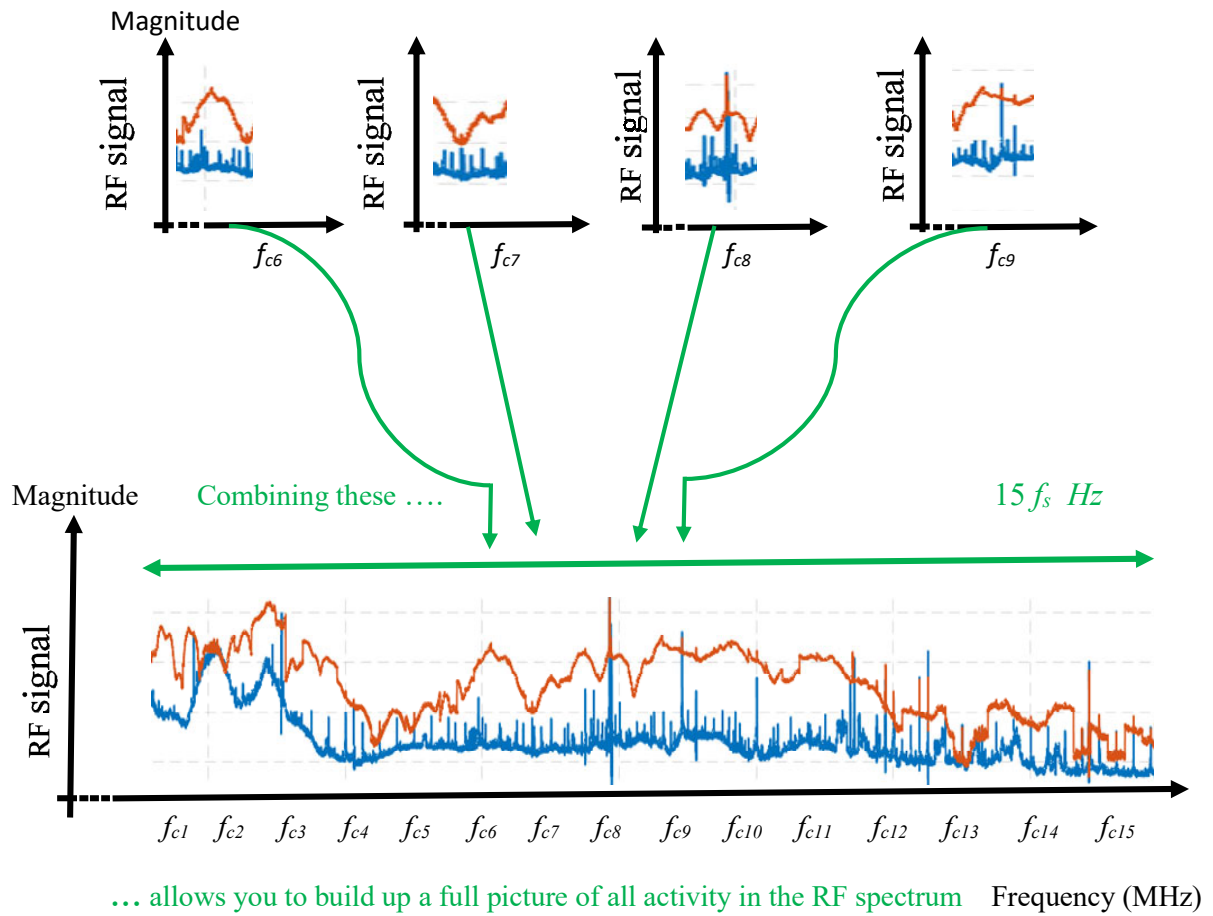


Fig. 3. Swept-FFT spectrum analysis, [18].

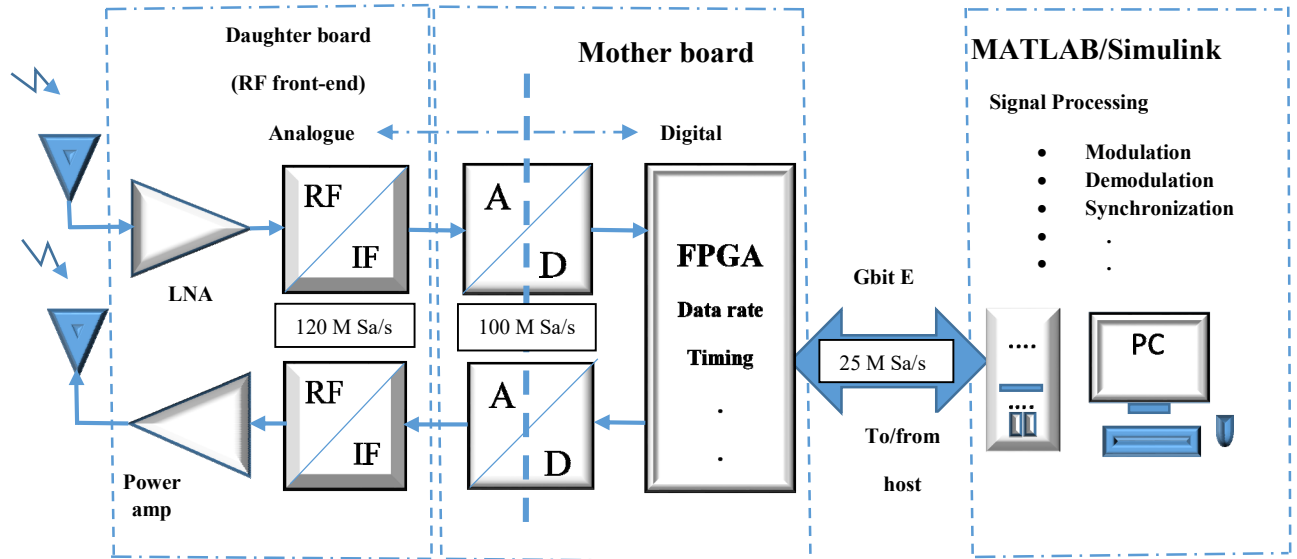


Fig. 4. USRP SDR system diagram.

Table 1. Most commonly used PD detection methods.

| PD detection methods | | | | |
|----------------------|---|--|--|--|
| Methods | Conventional methods | Non-Conventional methods | | |
| | Electrical method (IEC60270) | Optical method | Radiometric method/ UHF method | Acoustic method |
| Approach | -Detection and measurement of the apparent charge in pC. | -Detection of optical occurrences. | Detection of electromagnetic transients in - HF/VHF 3-300 MHz. - UHF 300-3000 MHz. | Detection of acoustic emissions from 10 kHz to 300 kHz. |
| Advantages | Suitable in laboratory environment. Has good sensitivity and accuracy. | Not affected by electromagnetic interference. Easy to measure. | Continuous monitoring in real time with good accuracy. PD source can be localized. | Real-time measurements. PD source can be localized. Immune to electromagnetic noise. |
| Disadvantages | Not suitable in real environment as it is sensitive to noise and very difficult to use on site. | Weak immunity against other light interferences. | Weak immunity against electromagnetic interferences. | Weak immunity against other acoustic interferences. |
| Computational burden | Low | Medium | Medium | High |
| Cost | Relatively expensive | Low cost | Relatively expensive, except for SDR | Low cost |
| Detection error | Small | Medium | Medium | Large |

Table 2. Comparison of SDR-based UHF sensing against a conventional portable spectrum analyser solution.

| Feature | USRP N200 | Portable Rohde & Schwarz FSH-8 Spectrum analyzer |
|-----------------------|---------------------------------|--|
| Cost | £600-1800 | £8k-15k |
| Size | Small | Medium |
| Reliability | High | Very high |
| Dynamic range | 80 dB for the ADC | 146 dB |
| Sensitivity | Medium | High |
| Frequency Range | 50MHz to 2200 MHz | 9 kHz to 8 GHz |
| Seamless capturing | No | Yes |
| Power Consumption (W) | 6 V, 2.4 A | 7.2V, 1.5A |
| Weight | 1.2 kg | 3 kg |
| Principle advantage | Reliability, accuracy, and cost | Reliability and accuracy |

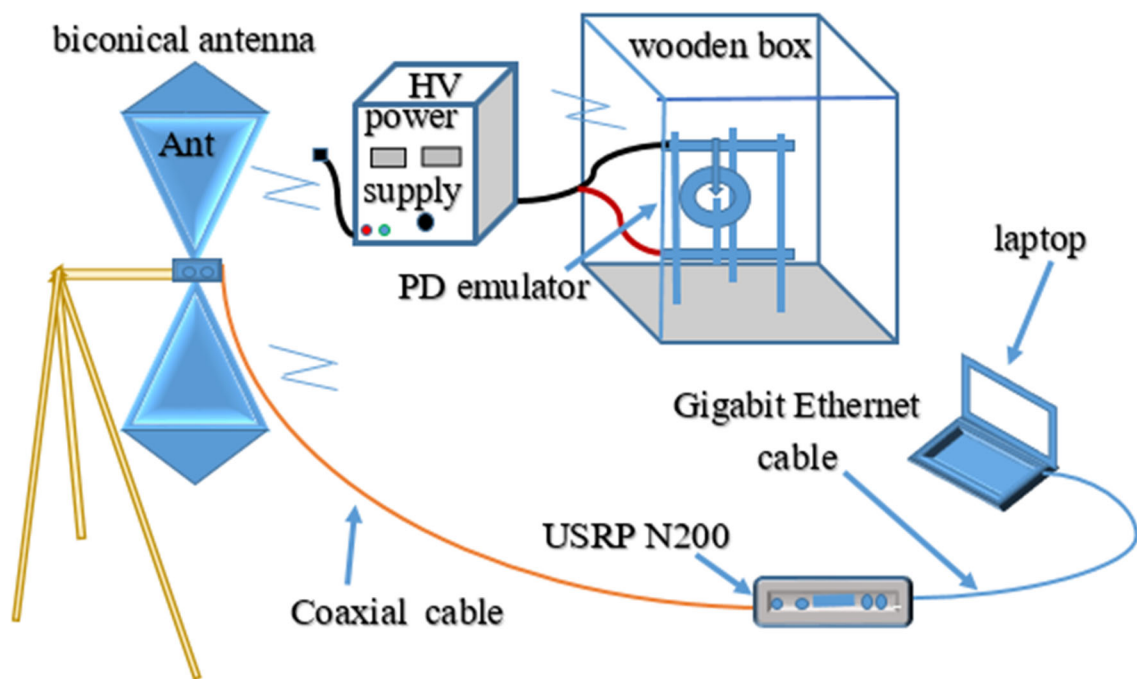
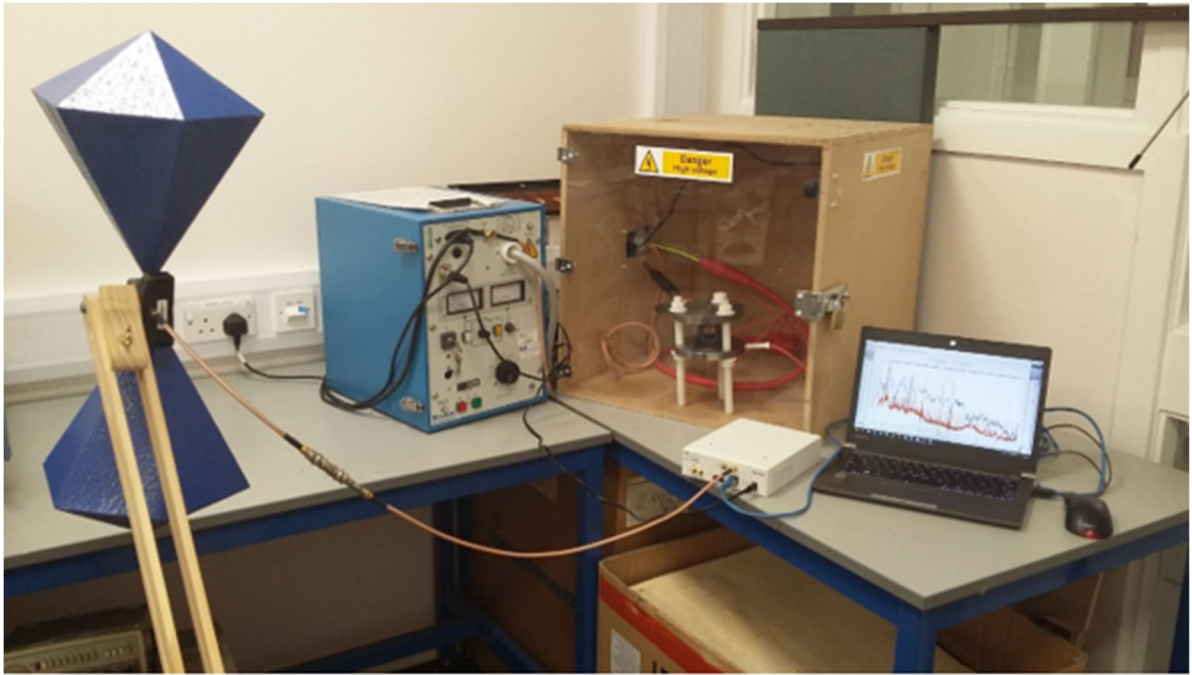


Fig. 5. Photo and diagram of the experimental setup.

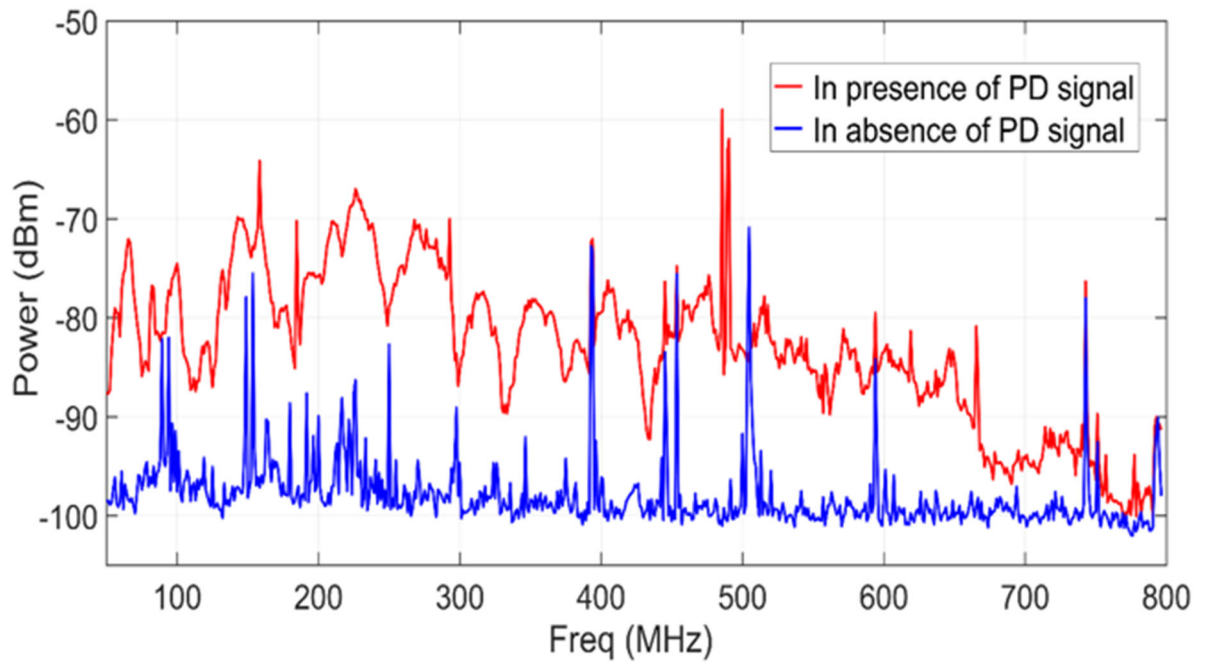
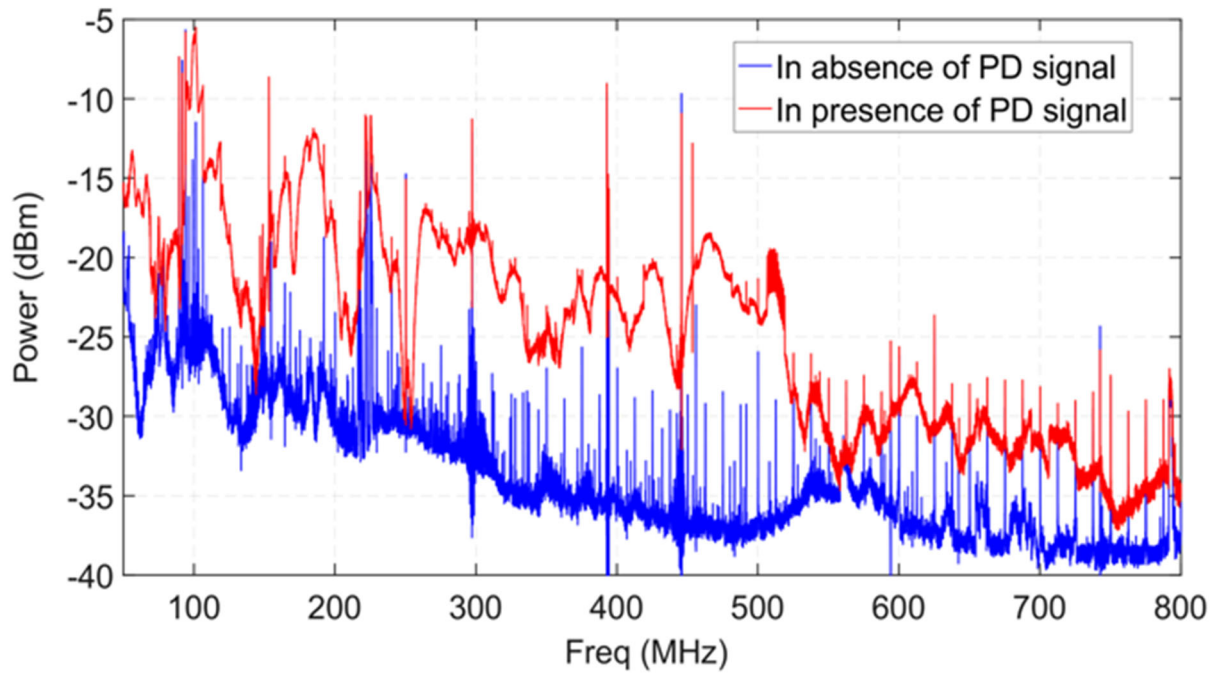


Fig. 6. Measured spectra indoors using USRP receiver (top) and spectrum analyzer (bottom).

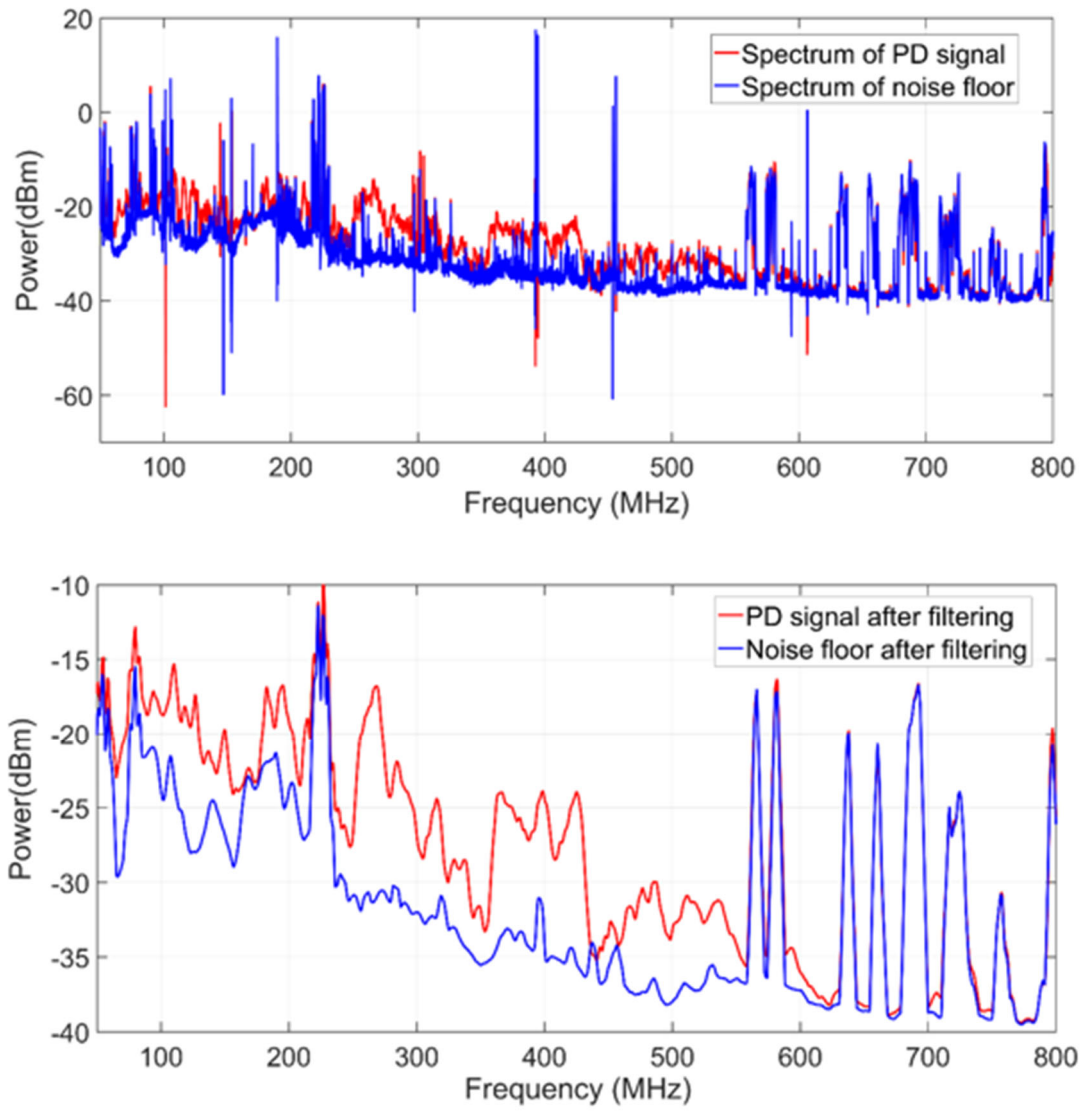


Fig. 7. Measured spectra using USRP outdoors before and after signal processing (uncalibrated).

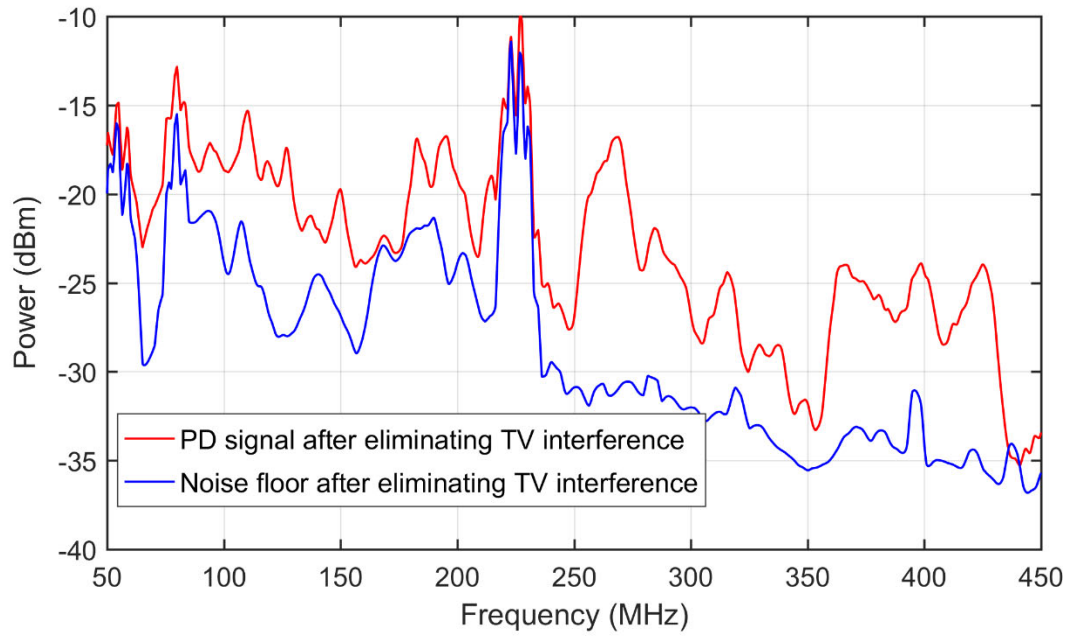


Fig. 8. PD signal and background noise plus interference after removing TV interference.

Table 3. Power values at the receiver locations (uncalibrated).

| Receiver location | Relative power in milliWatts |
|-------------------|------------------------------|
| 1 | 14.8 |
| 2 | 10.4 |
| 3 | 14.3 |
| 4 | 32.0 |
| 5 | 2.6 |
| 6 | 8.1 |

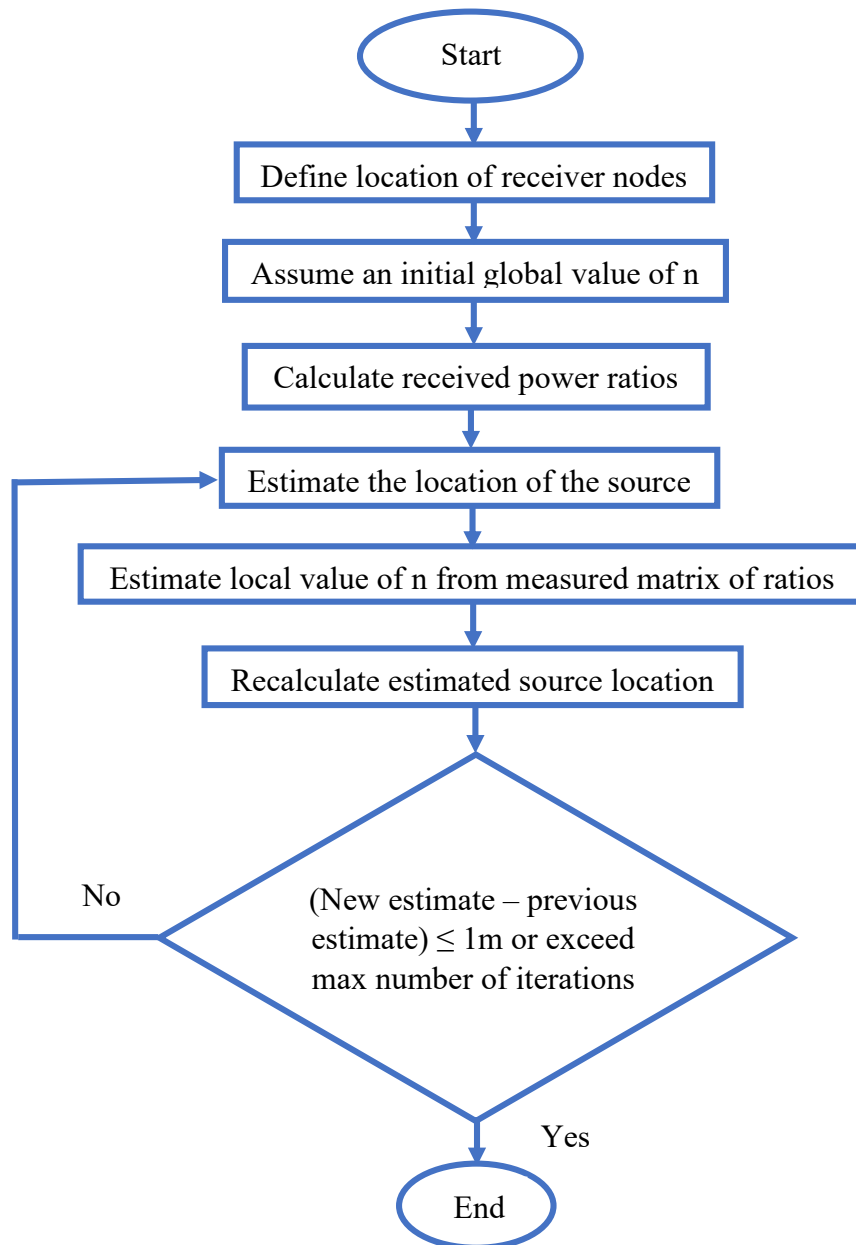


Fig. 9. Flowchart of the RSS localization algorithm.

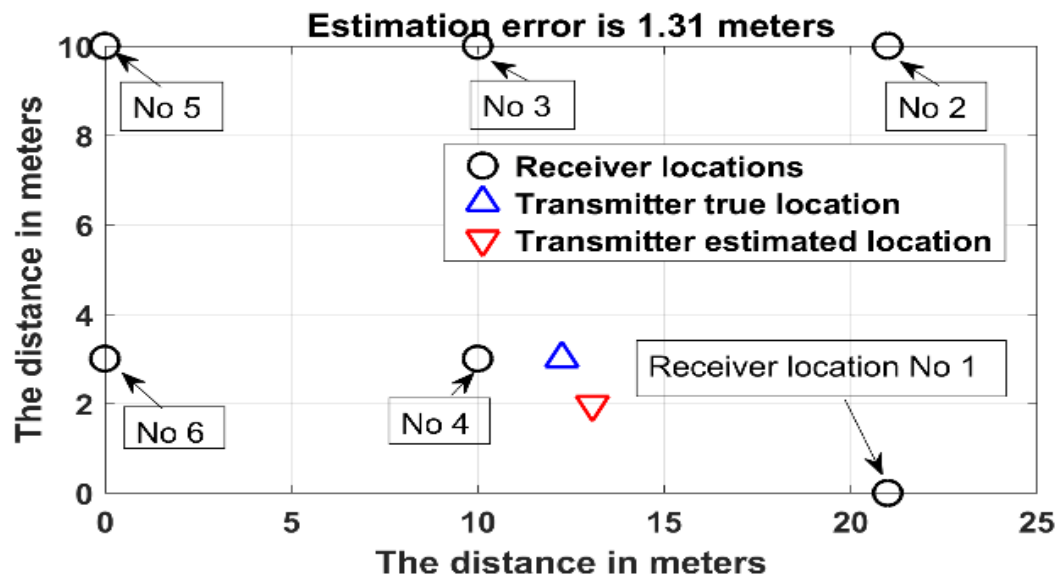


Fig. 10. PD source localization results.